

Supplementary Information

Microwaves-induced epitaxial growth of urchin-like MIL-53(Al) crystals on ceramic supports

Limor Ben Neon¹, Martin Drobek¹, Mikhael Bechelany^{1,2}, Bertrand Rebiere³, Anne Julbe^{1*}

¹Institut Européen des Membranes (IEM); Univ Montpellier, CNRS, ENSCM, Place Eugène Bataillon; 34095 Montpellier; France

²Gulf University for Science and Technology, GUST, Kuwait

³UAR Plateforme d'Analyses et Caractérisations (PAC) Chimie Balard Montpellier, Univ Montpellier, CNRS, ENSCM, Place Eugène Bataillon; 34095 Montpellier; France

*corresponding author: anne.julbe@umontpellier.fr

The ALD reactor chamber contains a heated circular sample holder ($\varnothing = 83$ mm) that can accommodate samples up to 10 mm high ($V_{\text{chamber}} = 54$ cm³). Five pieces of SiC foams (0.5 x 1.5 x 1.5 cm) were introduced simultaneously into the reactor chamber for alumina deposition. The chamber was connected to an Ar line, precursor vessels and to a rotary pump to achieve a pressure of $\sim 10^{-2}$ mbar. The injection of precursors was regulated by the aperture time of the precursor vessels, controlled by automatic valves. The introduction pressures of trimethylaluminum and H₂O were 10 mbar and 30 mbar respectively.

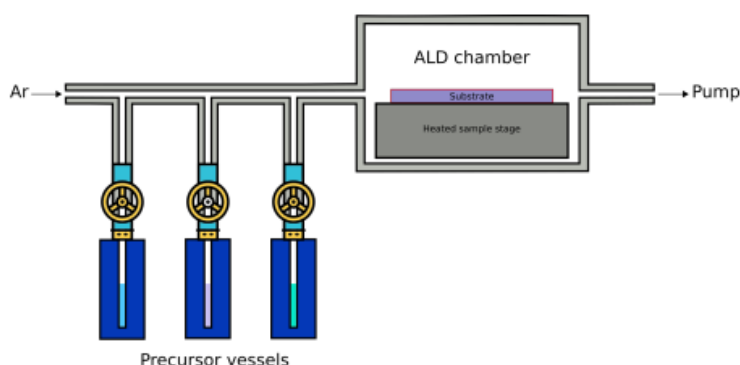


Figure S1: Schematic of the home-made ALD set-up developed for Al₂O₃ deposition (Octavio Graniel Tamayo, Atomic layer deposition for biosensing applications, PhD thesis- University of Montpellier-France, 2020).

Raman analysis was carried out to confirm the formation of MIL-53(Al) on SiC foam after hydrothermal synthesis by conventional or MW-assisted heating (Figure S2).

It should be noted that the foam has a very wavy surface and the amount of MIL-53(Al) relative to SiC is too low to be detected by X-ray diffraction.

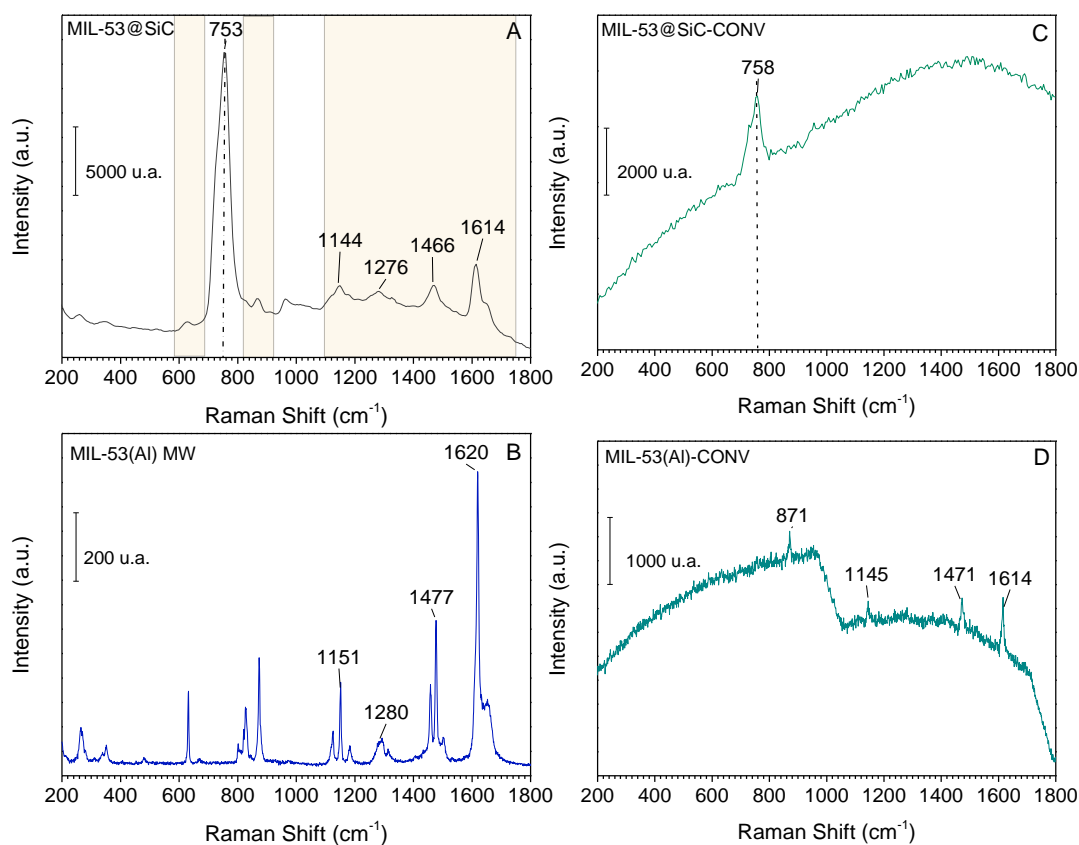


Figure S2: Raman spectra of MIL-53@SiC prepared using MW-assisted heating (A) and MIL-53@SiC-CONV prepared via conventional heating (B), in comparison with the Raman spectra of MIL-53(AI) powder synthesized under MW-assisted (C) and conventional heating (D). The band around 753 cm^{-1} corresponds to $\nu(\text{Si-C})$ of the SiC foam. The regions of spectra (A) highlighted in yellow correspond to MIL-53(AI) in which the bands of spectra A and B overlap and subsequently indicate the presence MIL-53(AI) supported on SiC. In the case of spectrum C, luminescence does not allow further interpretation of the spectrum above 1800 cm^{-1} . Thus, the vibration bands of MIL-53(AI) prepared via conventional heating could not be observed. Moreover, via the conventional heating method, MIL-53(AI) appears less crystallized. Its spectrum (D) is less defined, making its analysis more tedious.

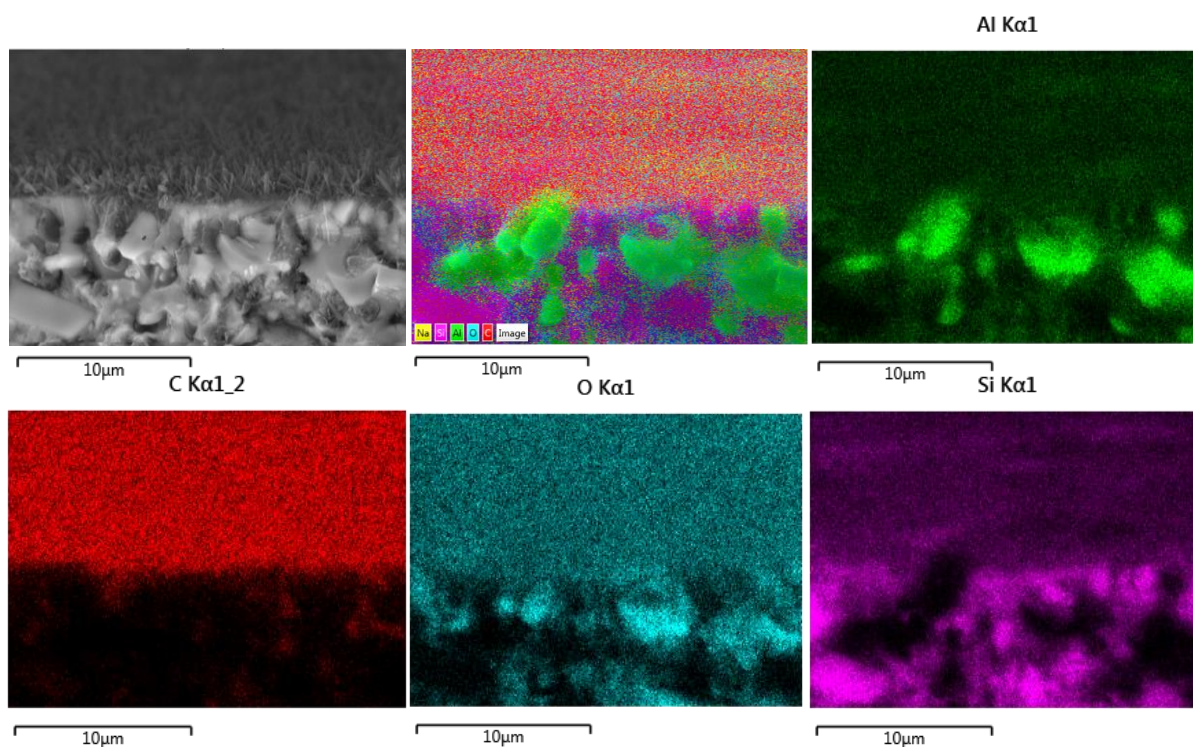


Figure S3: EDX mapping on the cross-section of MIL-53@SiC sample showing the dispersion of Al, C, O and Si atoms.

Table S1 : Dielectric properties and thermal conductivity of water, SiC, ZrO₂, Al₂O₃ and MIL-53(Al) precursors, at 2.45 GHz and room temperature. The dielectric constant is the ability to store electric charges while the dielectric loss is the capacity to transform the electromagnetic energy into heat.

Compound	Dielectric constant ϵ'	Dielectric loss ϵ''	Thermal conductivity (W/mK)	Ref
Water	78.68	10.61	0.609	1,2
Al(NO ₃) ₃ 500 mM	58.85	64.58	-	1
Al(NO ₃) ₃ 5 mM	80	20	-	1
Terephthalic acid	2.53	0.03	-	1
Terephthalic in complex with cation	70-77	14-29	-	1
Al ₂ O ₃	10.8	0.16	26	2
SiC	26.66	27.99	40	2
ZrO ₂	22.5	0.02	1.7	3

1. Laybourn, A. *et al.* Understanding the electromagnetic interaction of metal organic framework reactants in aqueous solution at microwave frequencies. *Phys. Chem. Chem. Phys.* **18**, 5419–5431 (2016).
2. Samanta, S. K., Basak, T. & Sengupta, B. Theoretical analysis on microwave heating of oil-water emulsions supported on ceramic, metallic or composite plates. *Int. J. Heat Mass Transf.* **51**, 6136–6156 (2008).
3. Yi, M. *et al.* Surface-enhanced raman scattering activity of zro2 nanoparticles: Effect of tetragonal and monoclinic phases. *Nanomaterials* **11**, (2021).

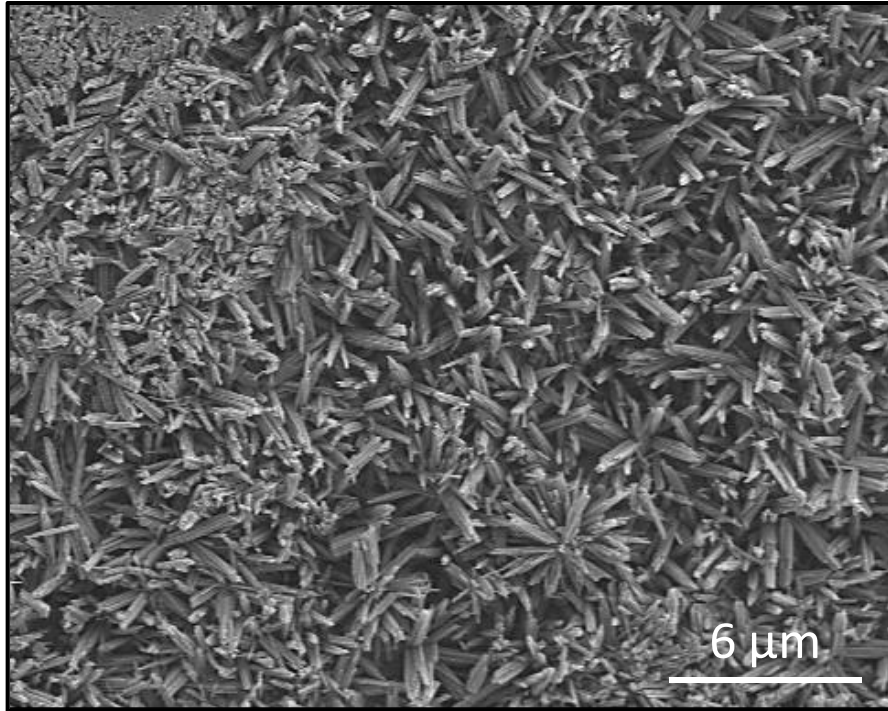


Figure S4: SEM image of a sample prepared by MW-assisted conversion of a γ -alumina Accu[®]spheres into MIL-53(Al) showing 1D-directional growth of urchin-like crystals.

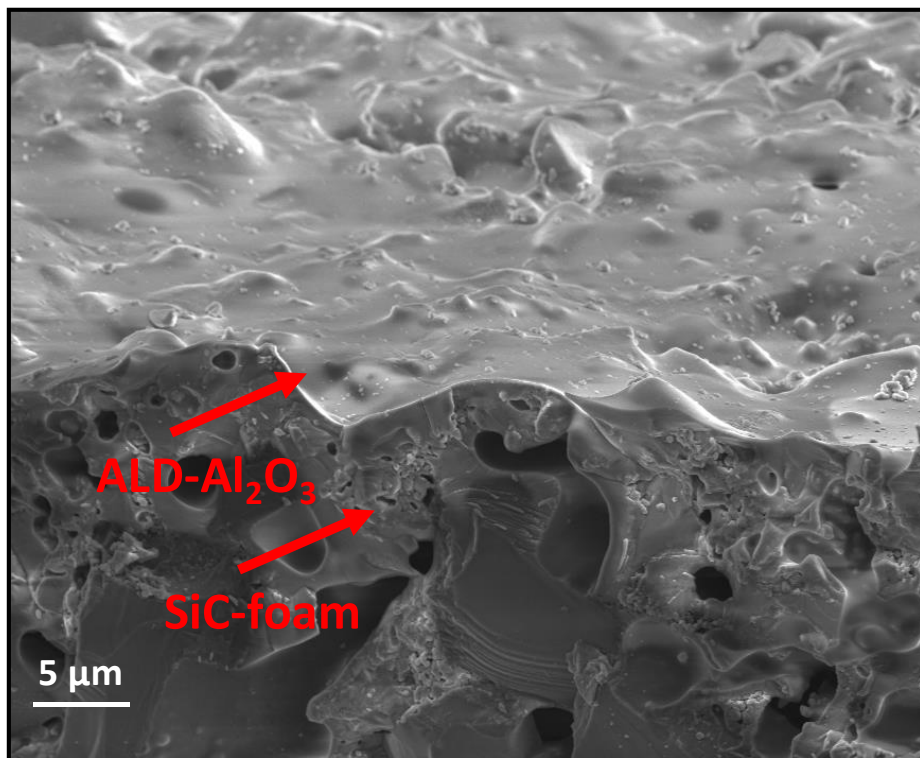


Figure S5: Cross-section of ALD-alumina coated SiC-foam.

Table S2: Elemental analysis result obtained by EDX of ALD-alumina coated SiC-foam in cross-section as presented in Figure S4 showing the difference in weight percentage of C, Na, O and Al (*note that the native SiC-foam contains an aluminum additive ~ 5 wt%).

wt% of elements probed via EDX	SiC-foam	ALD-alumina coating
O	22.3 ± 4.5	17.6 ± 3.5
Na	0.5 ± 0.1	-
Al	5.1* ± 1.0	12.3 ± 2.5
Si	31.7 ± 6.4	7.2 ± 1.4

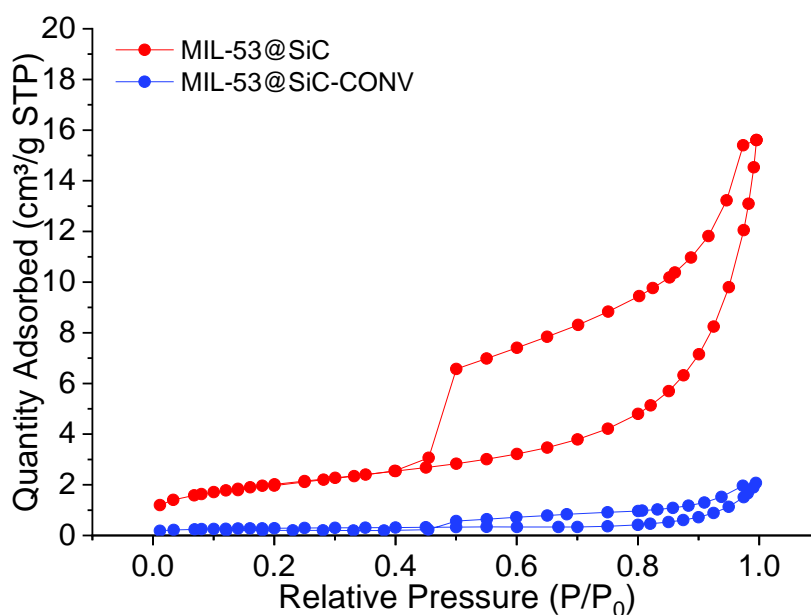


Figure S6: N₂ adsorption/desorption isotherms for MIL-53@SiC prepared under MW-assisted heating and MIL-53@SiC-CONV prepared under conventional heating.

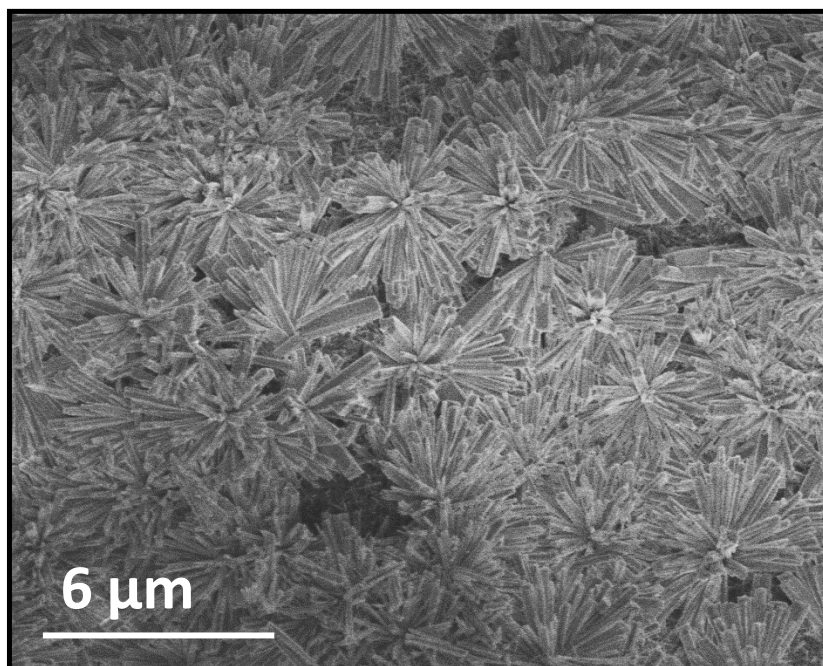


Figure S7: SEM images of MIL-53@SiC after adherence test, confirming good adhesion and unchanged distribution of MIL-53(AI) crystals on the ceramic supports.

Table S3: Results of sonication stability tests- Comparison of average aluminum concentration (EDX analysis- wt%) and sample mass variation before and after sonication.

	[Al] _{EDX} wt%	[Al] mass variation (wt%)
Before sonication	5.00 ± 0.5	-
After 15 min sonication	4.60 ± 0.5	- 0.40
After 60 min sonication	4.58 ± 0.5	- 0.42

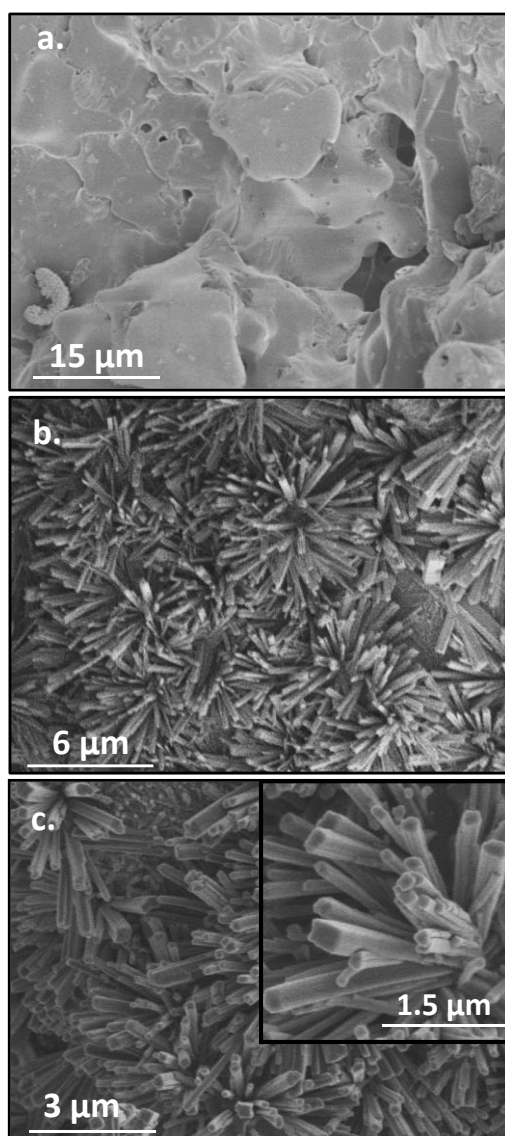


Figure S8: SEM images of pristine ZrO_2 foam (a) and MIL-53(Al) crystals grown on ZrO_2 foam by conversion of ALD-alumina (b, c) using the same synthesis procedure as for MIL-53@SiC. The ZrO_2 foams with 10 ppi were supplied by EPMF-France (reference: STELEX-ZrO2-10 PPI).

The nature of the ceramic support does not influence the textural properties of the formed MIL-53(Al) crystals. Indeed, the specific surface areas (S_{BET}) and pore volumes (V_p) measured for MIL-53(Al) grown on ZrO_2 and SiC were very similar (Table S4).

Table S4 : Comparison of the textural characteristics measured for MIL-53(Al) grown on SiC and ZrO_2 ceramic foams and extrapolated to the MIL-53(Al) material- Values of S_{BET} and pore volume (V_p) were attributed to the sole contribution of the MOF material (An error of ~10% is estimated for S_{BET} , V_p values)

Sample	Δm (wt%)*	S_{BET} (m^2/g)	V_p (cm^3/g)	S_{BET} (MIL-53(Al)) (m^2/g)	V_p (MIL-53(Al)) (cm^3/g)
MIL-53@ ZrO_2	1.1 %	1	0.002	91	0.182
MIL-53@SiC	9.1 %	7	0.019	80	0.200

$$*\Delta m = m_{(\text{sample after conversion})} - m_{(\text{pristine foam})}$$

Table S5 : Impact of thermal treatment of MIL-53@SiC (3h at 1000°C - 5°C/min- in air) on its textural characteristics.
 a. $\Delta m = m(\text{thermal treated MIL-53@SiC}) - m(\text{foam})$ b. wt% of Al_2O_3 determined by EDX. c. Mean pore size values at maximal distribution intensity. * S_{BET} and V_p determined by considering the wt% of the formed material (Al_2O_3) determined by EDX. (An error of ~10% is estimated on the S_{BET} , V_p).

	Δm (wt%) ^a	S_{BET} (m ² /g)	V_p (cm ³ /g)	Formed material	S_{BET} (formed material) (m ² /g)	V_p (formed material) (cm ³ /g)
As prepared in this work MIL- 53@SiC	9.1%	7	0.019	MIL-53(Al)	80	0.200
After calcination at 1000°C	2.7 % 3.5 % ^b	8	0.024	Al_2O_3	298 227*	0.926 0.681*

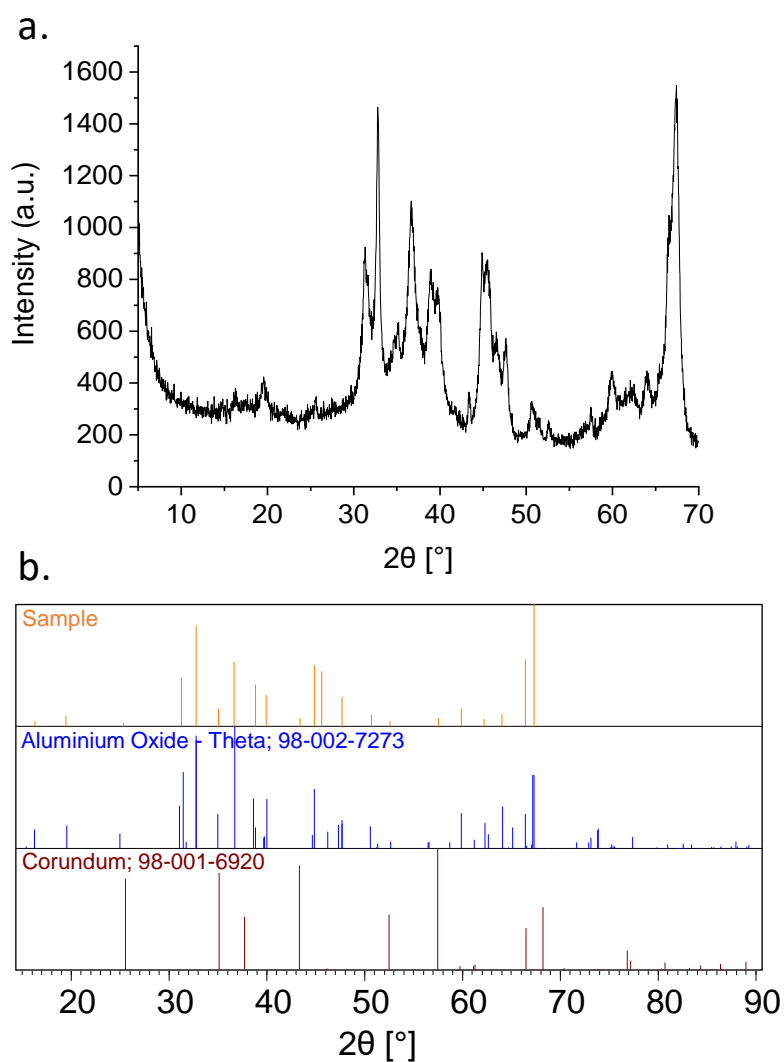


Figure S9: (a) PXRD diffraction pattern of Al_2O_3 obtained after calcination of MIL-53(Al) at 1000°C in air. Since XRD analysis was not feasible on foam samples, MIL-53(Al) was directly grown on 1g boehmite powder (Sasol) using the same synthesis conditions. The pattern was recorded with a Malvern Panalytical X'Pert Powder S using a scan rate of $0.021^\circ/\text{s}$. Diffractogram was analyzed with the software X'Pert Highscore Plus. Based on phase analysis (b), a major theta alumina phase and a minor corundum (alpha) alumina phase were determined with the respective proportion of 90% and 10% respectively.